Macropinocytosis of the PDGF β-receptor promotes fibroblast transformation by H-RasG12V

C. Schmees[a,*,†], R. Villaseñor[b,*], W. Zheng[a,‡], H. Ma[a], M. Zerial[b], C.-H. Heldin[a], and C. Hellberg[a,‡]
[a]Ludwig Institute for Cancer Research, Science for Life Laboratory, Uppsala University, SE-751 24 Uppsala, Sweden; [b]Max Planck Institute of Molecular Cell Biology and Genetics, 01307 Dresden, Germany

ABSTRACT Receptor tyrosine kinase (RTK) signaling is frequently increased in tumor cells, sometimes as a result of decreased receptor down-regulation. The extent to which the endocytic trafficking routes can contribute to such RTK hyperactivation is unclear. Here, we show for the first time that fibroblast transformation by H-RasG12V induces the internalization of platelet-derived growth factor β-receptor (PDGFRβ) by macropinocytosis, enhancing its signaling activity and increasing anchorage-independent proliferation. H-RasG12V transformation and PDGFRβ activation were synergistic in stimulating phosphatidylinositol (PI) 3-kinase activity, leading to receptor macropinocytosis. PDGFRβ macropinocytosis was both necessary and sufficient for enhanced receptor activation. Blocking macropinocytosis by inhibition of PI 3-kinase prevented the increase in receptor activity in transformed cells. Conversely, increasing macropinocytosis by Rabankyrin-5 overexpression was sufficient to enhance PDGFRβ activation in nontransformed cells. Simultaneous stimulation with PDGF-BB and epidermal growth factor promoted macropinocytosis of both receptors and increased their activation in nontransformed cells. We propose that H-Ras transformation promotes tumor progression by enhancing growth factor receptor signaling as a result of increased receptor macropinocytosis.

INTRODUCTION

Receptor tyrosine kinases are frequently overactivated in human tumors as a result of point mutations, amplifications, or overexpression of ligand (Zwick et al., 2001). In addition, transforming mutations causing delayed or impaired internalization and degradation of activated growth factor receptors have been reported (Peschard

and Park, 2003). Mutations in the endocytic machinery have also been detected (Bache et al., 2004), including inactivation of the tumor suppressor Tsg101, which inhibits sorting of activated receptors toward lysosomal degradation. The viral oncogene product v-Cbl prevents receptor ubiquitination and degradation, thereby promoting transformation of human cells. The effects of impaired receptor down-regulation are best described for the ErbB subfamily (Roepstorff et al., 2008). Thus epidermal growth factor receptor (EGFR) deletion mutants lacking the Cbl-binding site are frequently found in glioblastomas (Frederick et al., 2000; Peschard and Park, 2003), whereas HER2, which is overexpressed in 20–30% of breast cancers (Slamon et al., 1987), is resistant to degradation (Roepstorff et al., 2008).

Members of the Ras subfamily of GTPases are mutated in ~20% of human malignancies (Karnoub and Weinberg, 2008). Through activation of, for example, Raf/Erk/mitogen-activated protein kinase (MAPK), phosphatidylinositol (PI) 3-kinase/Akt, and RALGDS pathways (Downward, 2003; Karnoub and Weinberg, 2008), Ras proteins promote important cellular functions, including cell survival, cell-cycle progression, and cytoskeletal rearrangements. In addition to these events, oncogenic H-Ras (Bar-Sagi and Feramisco, 1986; Porat-Shliom et al., 2008) and K-Ras (Amyere et al., 2000) induce

macropinocytosis. Macropinocytosis is a form of clathrin- and dynamin-independent endocytosis in which PI 3-kinase–dependent (Amyere *et al.*, 2000; Schnatwinkel *et al.*, 2004), actin-driven plasma membrane ruffling mediates uptake of fluids and large molecules (Kerr and Teasdale, 2009). It was recently shown that macropinosomes contain active H-Ras (Porat-Shliom *et al.*, 2008), suggesting that these vesicles might constitute a platform for signaling. Several membrane proteins, including CD44 and ICAM-1, are transported through macropinosomes (Eyster *et al.*, 2009). Although growth factors such as platelet-derived growth factor (PDGF; Davies and Ross, 1978) and epidermal growth factor (EGF; West *et al.*, 1989) induce macropinocytosis, their activated receptors are mainly internalized through clathrin- or caveolin-mediated endocytosis. However, it was recently demonstrated that ErbB3 translocation to the nucleus in prostate carcinoma cells was abrogated by inhibition of macropinocytosis (Koumakpayi *et al.*, 2011), suggesting a role for macropinocytosis in tumor cell signaling.

PDGF isoforms are major mitogens for a number of cell types, including mesenchymal cells such as fibroblasts and smooth muscle cells, and overactivity of PDGF signaling has been linked to the development of atherosclerosis, fibrotic diseases, and malignancies (Andrae *et al.*, 2008). The PDGF family consists of four polypeptide chains: the classic PDGF A and B chains and the more recently described PDGF C and D chains, which act by binding to the structurally related α- and β-protein tyrosine kinase receptors. On ligand-induced dimerization, activated receptor tyrosine kinases are internalized and transported through early endosomes before being either recycled to the plasma membrane or sorted to late endosomes and lysosomes for degradation. Internalized receptors are associated with downstream effectors, providing both spatial and temporal regulation of the assembled signaling complexes (Disanza *et al.*, 2009; Murphy *et al.*, 2009; Rodahl *et al.*, 2009; Sadowski *et al.*, 2009). Thus regulation of the subcellular localization of receptors and substrates has been postulated to provide an additional level of regulation of cellular responses to growth factors.

Increased expression of PDGF isoforms and receptors during tumor progression has been reported in gliomas (Hermanson *et al.*, 1992; Calzolari and Malatesta, 2010), hepatocellular carcinomas (Gotzmann *et al.*, 2006; Fischer *et al.*, 2007), and metastatic mammary cancers (Jechlinger *et al.*, 2006), as well as in follicular and papillary thyroid carcinoma cell lines (Chen *et al.*, 2006). Although aberrant PDGF receptor (PDGFR) activity causes transformation, the importance of wild-type PDGFR activation in cells transformed by other oncoproteins has not been described. In the present study, we show that the anchorage-independent proliferation of H-RasG12V–transformed fibroblasts depends on PDGFR signaling. Moreover, H-RasG12V increased the PDGFRβ phosphorylation and downstream signaling by promoting receptor internalization through macropinocytosis. The increased PDGFRβ activation observed was further enhanced by EGFR activation, indicating that receptor tyrosine kinase cross-talk may occur through macropinocytosis of activated receptors, which results in increased and prolonged receptor activation.

RESULTS
PDGF receptor activation promotes anchorage-independent growth of H-RasG12V–transformed fibroblasts
To investigate whether activation of PDGFRβ contributes to H-Ras transformation, we grew immortalized human fibroblasts transformed with H-RasG12V in soft agar in medium supplemented with 3% fetal bovine serum (FBS; Figure 1A). The H-RasG12V fibroblasts

readily formed colonies under these conditions. The growth in soft agar was dependent on PDGF receptor kinase activity, since it was inhibited by the PDGFRβ kinase inhibitors AG1296 (Figure 1A) and imatinib (Supplemental Figure S1). In contrast, proliferation of cells grown on plastic was not inhibited by AG1296 (Supplemental Figure S1). Furthermore, addition of 50 ng/ml PDGF-BB increased colony formation, demonstrating that PDGF signaling promotes the growth of H-Ras–transformed fibroblasts. Under these conditions, colony growth of nontransformed immortalized human fibroblasts was not observed (unpublished data).

Increased PDGFRβ signaling in H-RasG12V–transformed fibroblasts
To determine which signaling pathways are important for the effect of PDGF on H-Ras transformation, the activation of PDGF receptors in transformed cells and parental cells was compared. The amplitude and duration of receptor tyrosine phosphorylation were increased in H-RasG12V–transformed fibroblasts (Figure 1B). The increase occurred on most known autophosphorylation sites and particularly on Y1021 (Supplemental Figure S2). In the analysis of the major downstream signaling pathways, the phosphorylation of Akt, phospholipase Cγ (PLCγ), and the protein kinase C (PKC) substrate MARCKS was increased in H-Ras–transformed cells, whereas Erk1/2 phosphorylation was not affected (Figure 1B; quantifications in Supplemental Figure S3). Thus the increased PDGFRβ phosphorylation observed after H-RasG12V transformation leads to a selective increase of signaling via certain downstream pathways.

H-RasG12V transformation promotes PDGFRβ internalization through macropinocytosis
Ras coordinates multiple signaling pathways (Mitin *et al.*, 2005), and so we next investigated the molecular mechanism underlying the increased PDGFRβ activation in H-RasG12V-transformed fibroblasts. Because oncogenic H-Ras alters membrane trafficking by increasing macropinocytosis (Bar-Sagi and Feramisco, 1986; Porat-Shliom *et al.*, 2008), we investigated whether the observed increase in PDGFRβ activity could be explained by H-RasG12V–induced changes in receptor trafficking. To determine whether PDGF receptor endocytosis is altered in H-Ras–transformed cells, we stimulated fibroblasts with PDGF-BB and monitored the simultaneous internalization of PDGFRβ and uptake of high–molecular mass (70,000 Da) Texas Red-dextran. In these fibroblasts, H-RasG12V transformation alone induced minor levels of dextran uptake during the course of this experiment (Figure 2A). Consistent with a previous report, PDGF-BB induced dextran uptake into large vesicles (Davies and Ross, 1978) in both cell lines, a process that was abrogated by inhibition of PI 3-kinase (Figure 2A). After stimulation, PDGFRβ colocalized with vesicles containing Texas Red-dextran (Figure 2A), but the proportion of receptor found in these vesicles was much larger after H-RasG12V transformation (Figure 2B).

Characterization of PDGFRβ-containing macropinosomes
Dextran uptake may also occur through other modes of endocytosis (Hewlett *et al.*, 1994). To further characterize the PDGFRβ- and dextran-containing vesicles, we stained cells for the Rab5 effector Rabankyrin-5, which localizes to macropinosomes (Schnatwinkel *et al.*, 2004; Figure 2C). H-RasG12V transformation induced a two-fold increase in the proportion of vesicles positive for PDGFRβ, dextran, and Rabankyrin-5 (Figure 2D and Supplemental Figure S4). In contrast, the number of vesicles positive for PDGFRβ, dextran, and EEA1, an early endosomal marker that is absent from immature macropinosomes (Kerr *et al.*, 2006), was not affected (Figure 2D
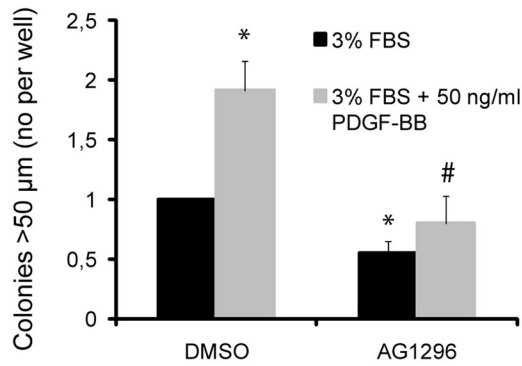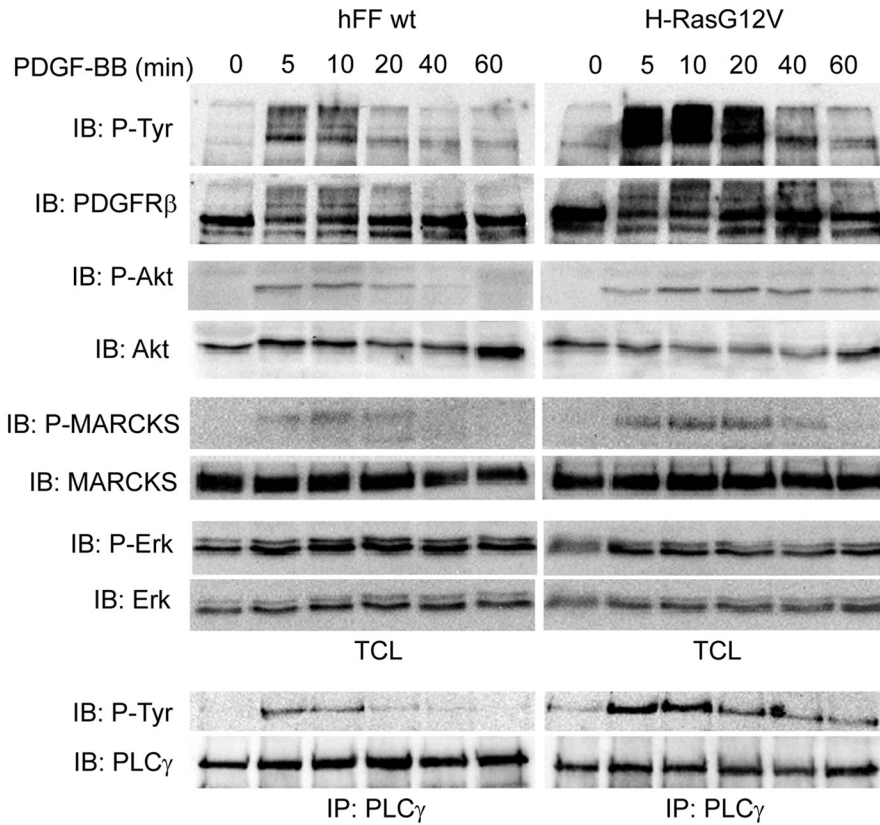
FIGURE 1: H-RasG12V transformation of fibroblasts results in increased PDGFRβ signaling that is required for growth in soft agar. (A) H-RasG12V–transformed fibroblasts were seeded in soft agar in medium containing 3% FBS. Where indicated, 50 ng/ml PDGF-BB with or without 2 μM of the PDGFRβ inhibitor AG1296 was added to the medium. After 5 d of incubation, the number of colonies >50 μm was counted. Data are given as means of three separate experiments ± SEM. Statistically significant (p < 0.05) differences compared with control cells (*) or PDGF-BB treated cells (#) are indicated. (B) Serum-starved cells were stimulated with 50 ng/ml PDGF-BB for the indicated time periods, and total cell lysates were collected. Where indicated, PLCγ was immunoprecipitated as described in *Materials and Methods*. Proteins were separated by SDS–PAGE, followed by immunoblotting using the indicated antibodies and visualization using a LAS-100plus CCD camera.

macropinosomes (Kerr and Teasdale, 2009).

To determine the fate of PDGFRβ internalized through macropinocytosis, we determined the kinetics of receptor trafficking toward late endosomes/lysosomes by staining cells for LAMP-1 and PDGFRβ. Although the amount of receptor colocalizing with LAMP-1 remained consistently higher in Ras-transformed cells, the kinetics of PDGFRb localization to LAMP-1–positive endosomes was identical between the cell lines (Figure 2F). During both clathrin- and caveolin-mediated endocytosis, the GTPase dynamin is required for vesicle fission, whereas macropinocytosis occurs independent of dynamin activation (Mayor and Pagano, 2007). To further verify that H-RasG12V transformation instigates a functional switch in receptor uptake, the dynamin dependence of PDGFRβ degradation was determined. Unlike in wt fibroblasts, the dynamin inhibitor dynasore did not significantly affect the degradation of PDGFRβ in H-RasG12V–transformed cells (Figure 2G), supporting the view that H-Ras transformation stimulated internalization of the receptor by macropinocytosis rather than by clathrin- or caveolin-mediated endocytosis. The dynamin-independent internalization was confirmed by immunofluorescence staining showing internalization of PDGFRβ in H-RasG12V–transformed, but not wt, fibroblasts transfected with dominant-negative dynaminK44A (Supplemental Figure S5).

Internalization through macropinocytosis increases PDGFRβ phosphorylation

To investigate whether macropinocytosis of PDGFRβ is required for the observed increase in receptor activation in H-RasG12V-transformed fibroblasts, we inhibited macropinocytosis pharmacologically (Figure 3A). Inhibition of PI 3-kinase using LY294002, as monitored by inhibition of Akt phosphorylation (Supplemental Figure S6), decreased the amplitude and duration of PDGFRβ phosphorylation in H-RasG12V–transformed fibroblasts (Figure 3A), which resembled the kinetics measured in wt cells. A small increase in receptor phosphorylation was observed in wt fibroblasts (Supplemental Figure S6), possibly due to the requirement for PI 3-kinase activity in intracellular receptor sorting (Petiot et al., 2003).

We next sought to enhance macropinocytosis by overexpressing Rabankyrin-5 (Schnatwinkel et al., 2004). As expected, overexpression of this protein enhanced receptor internalization into Rabankyrin-5–positive vesicles in wt fibroblasts (Figure 3B). Remarkably, this also almost doubled the relative receptor phosphorylation in both wt and H-RasG12V–transformed fibroblasts (Figure 3, C and D), supporting the notion that macropinocytosis enhances receptor activation.

and Supplemental Figure S4). Low levels of large dextran- and PDGFRβ-containing vesicles positive also for Rabankyrin-5 were detected in wild-type (wt) fibroblasts (Figure 2D and Supplemental Figure S4), suggesting that H-RasG12V transformation enhances a normally occurring event. Consistent with the notion that PDGFRβ internalization occurred through macropinocytosis, the majority (84%) of the dextran-containing vesicles that also contained PDGFRβ were >0.2 μm (Figure 2E), which is a proposed minimum size of

However, although Rabankyrin-5 expression did not affect PDGFRβ expression levels, we consistently observed a decreased solubility of PDGFRβ in stimulated cells (Figure 3C and Supplemental Figure S4). Although Rabankyrin-5 overexpression enhanced the uptake of PDGFRβ into macropinosomes, downregulating Rabankyrin-5 with small interfering RNA only reduced the uptake of PDGFRβ into dextran-positive vesicles by 20% in Ras-transformed cells, indicating that Rabankyrin-5 is not required for receptor uptake into macropinosomes. This small but significant effect did not significantly reduce PDGFRβ phosphorylation (unpublished data).

Recycling of PDGFRβ in H-RasG12V–transformed fibroblasts

After internalization, macropinosomes can fuse back with either the plasma membrane or other endosomal compartments (Swanson and Watts, 1995; Porat-Shliom et al., 2008). To investigate whether H-RasG12V transformation altered the basal membrane trafficking in fibroblasts, we determined the trafficking of an antibody bound to cell surface PDGFRβ (Mitchell et al., 2004). After antibody binding and internalization, an acidic wash step removed cell surface–bound antibodies that had not been internalized. After
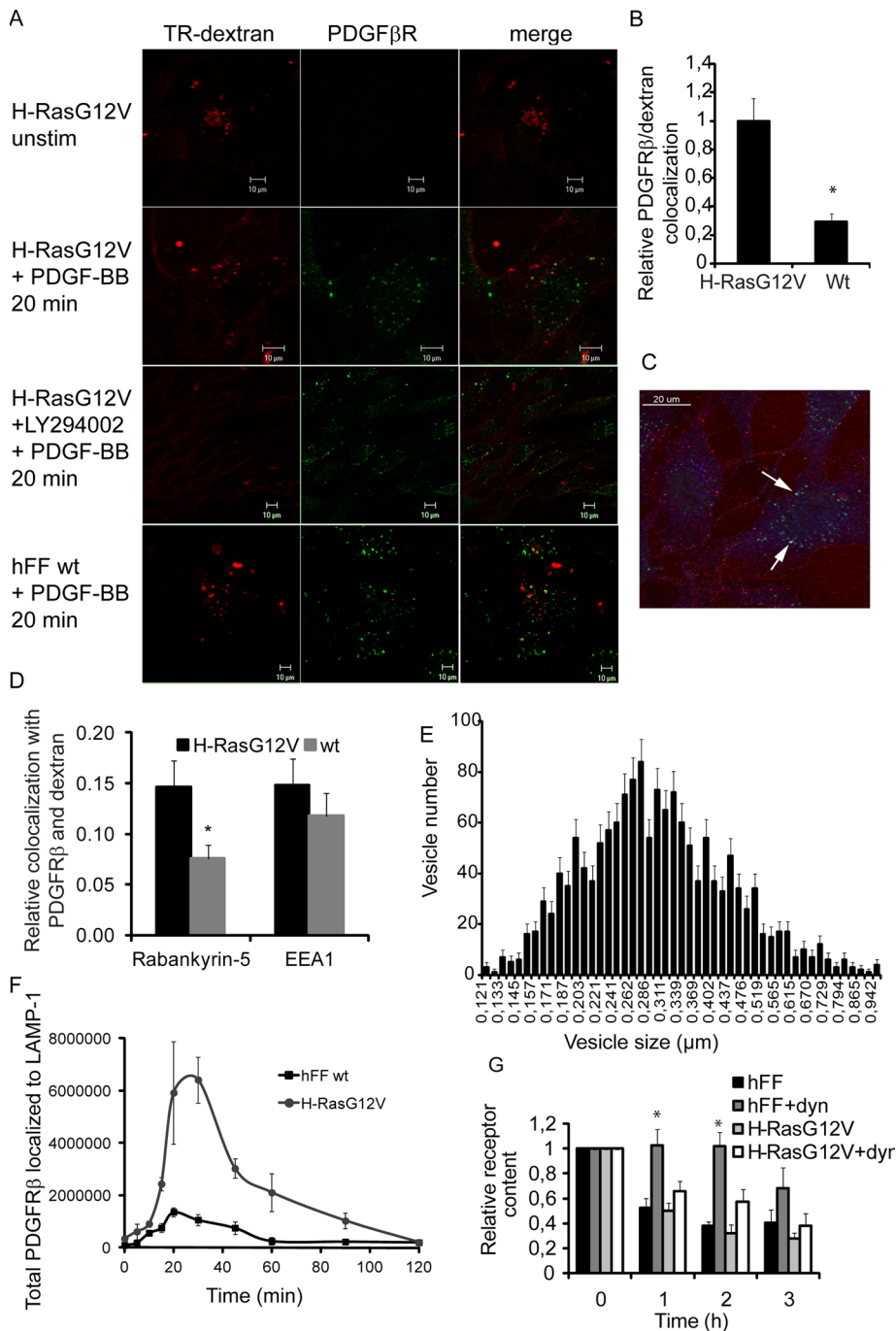
FIGURE 2: H-RasG12V transformation promotes ligand-activated PDGFRβ internalization through macropinocytosis. (A) H-RasG12V-transformed fibroblasts were preincubated with 25 μM LY294002 or vehicle (0.1% dimethyl sulfoxide [DMSO]) for 15 min. Wild-type or H-RasG12V–transformed fibroblasts were incubated with or without 50 ng/ml PDGF-BB for 20 min in the presence of 1 mg/ml Texas Red-dextran (TR-dextran; MW, 70,000 Da). The subcellular localization of PDGFRβ and dextran was examined by confocal microscopy. (B) H-RasG12V–transformed fibroblasts were stimulated with 50 ng/ml PDGF-BB for 10 min in the presence of 1 mg/ml Texas Red-dextran (MW, 70,000 Da). The relative amount of PDGFRβ colocalizing with dextran was calculated using the software MotionTracking as described in Materials and Methods. The graph shows normalized colocalization ± SEM from one experiment. Statistically significant difference was determined using unpaired Student's t test assuming equal variance: *p < 0.05. (C) H-RasG12V–transformed cells were stimulated with 50 ng/ml PDGF-BB in the presence of 1 mg/ml Texas Red-dextran (Red) as described and stained with antibodies recognizing Rabankyrin-5 (green) and PDGFRβ (blue). Arrows indicate vesicles containing all three markers. (D) Analysis of triple colocalization between EEA1 and Rabankyrin-5 with dextran and PDGFRβ was calculated using the software MotionTracking. At least 40 cells were imaged per time point. Data are given as mean ± SEM from one experiment. Statistically significant

difference was determined using unpaired Student's t test assuming equal variance: *p < 0.05. (E) H-RasG12V–transformed fibroblasts were incubated for 10 min with 1 mg/ml Texas Red-dextran (MW, 70,000 Da) and 50 ng/ml PDGF-BB. After washes with ice-cold PBS, the cells were fixed and stained with antibodies recognizing PDGFRβ. Images were acquired by confocal microscopy, and the mean size distribution of the dextran-containing vesicles colocalizing with PDGFRβ ± SEM in H-RasG12V–transformed fibroblasts was calculated using the software MotionTracking as described in Materials and Methods. (F) Cells were stimulated with 50 ng/ml PDGF-BB and stained with antibodies recognizing LAMP-1 and PDGFRβ. Colocalization between LAMP-1 and PDGFRβ was calculated using the software MotionTracking. At least 40 cells were imaged per time point. Data are given as mean ± SEM from one experiment. (G) Cells were incubated for 30 min with vehicle (0.2% DMSO) or 40 μM dynasore, followed by stimulation with 50 ng/ml PDGF-BB as indicated. Total cell lysates were separated by SDS–PAGE, and PDGFRβ was detected by immunoblotting. The mean relative receptor content ± SEM (n = 4) is shown. Statistically significant difference was determined using unpaired Student's t test assuming equal variance: *p < 0.05.
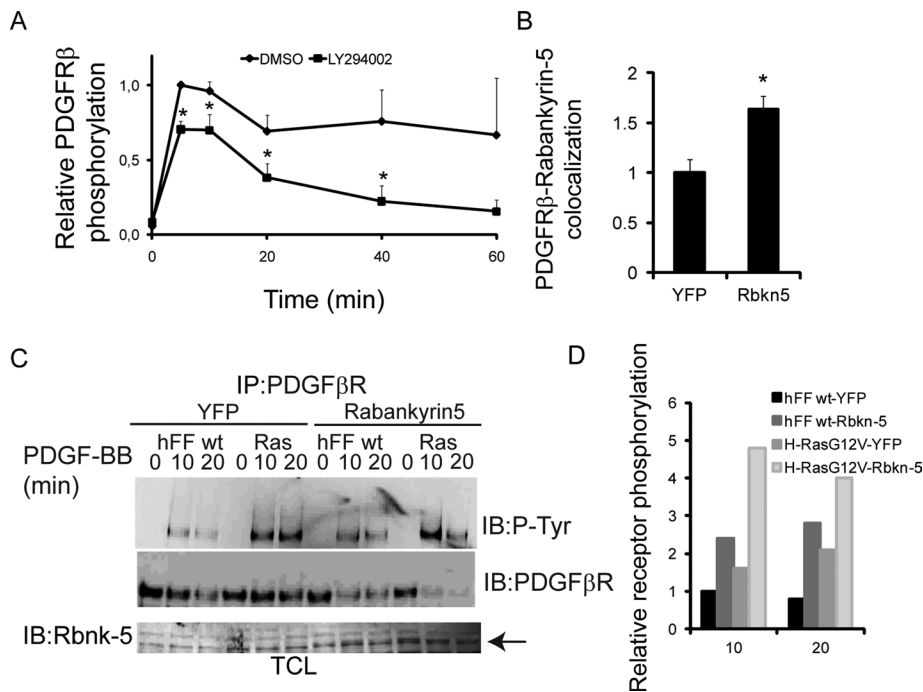
FIGURE 3: PDGFRβ internalization through macropinosomes enhances receptor activity. (A) Serum-starved, H-RasG12V–transformed fibroblasts were treated with 25 μM LY294002 or vehicle (0.1% DMSO) for 15 min, followed by stimulation with 50 ng/ml PDGF-BB for the indicated time periods. Total cell lysates were separated by SDS–PAGE, followed by immunoblotting, and normalized relative receptor phosphorylation is shown as means ± SEM. Statistically significant difference was determined using unpaired Student's *t* test assuming equal variance: *p < 0.05. (B) Wild-type fibroblasts were transfected with Rabankyrin-5–YFP or empty vector. Starved cells were stimulated with 50 ng/ml PDGF-BB for 20 min, fixed, and stained with antibodies recognizing Rabankyrin-5 and PDGFRβ. Colocalization was calculated using the software MotionTracking. At least 100 cells were imaged per time point. Data are given as mean ± SEM from three experiments. (C) Cells were transfected with Rabankyrin-5–YFP or empty vector. Starved cells were stimulated with 50 ng/ml PDGF-BB for the indicated time periods, and PDGFRβ was immunoprecipitated as described in *Materials and Methods*. Proteins were separated by SDS–PAGE, followed by immunoblotting using the indicated antibodies and visualization using a LAS-100plus CCD camera. After densitometry analysis, relative receptor phosphorylation was calculated, and the fold change compared with wt fibroblasts stimulated for 10 min is indicated. (D) Quantification of the data presented in C.

allowing time for receptor recycling, a subsequent incubation with an Alexa 488–labeled secondary antibody demonstrated that H-RasG12V caused the antibody–PDGFRβ complex to internalize and recycle back to the plasma membrane (Figure 4A). This shows that H-RasG12V transformation affects the intrinsic, slow membrane trafficking of the PDGFRβ in the absence of ligand.

To investigate whether also ligand-induced macropinocytosis would allow for receptor recycling, we determined the rate of clearance of PDGFRβ from the cell surface. In H-RasG12V–transformed fibroblasts, the rate of PDGFRβ clearance from the cell surface was decreased compared with wt fibroblasts (Figure 4B). This is in contrast to our finding that the receptor is internalized (Figure 2A), trafficked to late endosomes/lysosomes (Figure 2F), and degraded (Figure 2G). Because macropinosomes may fuse back with the plasma membrane, it appears likely that a pool of PDGFRβ is rapidly trafficked toward degradation, whereas another pool is recycled back to the plasma membrane from the macropinosomes to continue signaling. We previously showed that increased activation of PKC promoted Rab4a-dependent recycling of the PDGFRβ from an early endosomal compartment (Hellberg et al., 2009). Because we observed increased activation of PKC, as detected by elevated and prolonged phosphorylation

of MARCKS (Figure 1B), we investigated whether the observed PDGFRβ recycling from macropinosomes occurs through this pathway. However, down-regulation of PKC by overnight incubation with 1 μM phorbol 12-myristate 13-acetate (PMA) did not increase the rate of receptor clearance from the cell surface (Figure 4C). The shift toward receptor macropinocytosis and recycling was associated with a minor increase in receptor ubiquitination (Figure 4E and Supplemental Figure S2), indicating that H-RasG12V does not exert its effects on these events by altering receptor ubiquitination.

H-RasG12V does not promote macropinocytosis of activated EGFR

To evaluate whether other growth factor receptors are also internalized through macropinocytosis in H-RasG12V–transformed fibroblasts, we monitored internalization of EGFR concomitantly with uptake of Texas Red-dextran. However, EGF induced little or no colocalization between the EGFR and dextran in H-RasG12V–transformed fibroblasts (Figure 5A). This was confirmed in HeLa cells transiently transfected with H-RasG12V, in which the endocytosis of EGF-Alexa 555 and transferrin-Alexa 647 were followed by confocal microscopy. As shown in Figure 5B, H-RasG12V transformation did not affect the transport of EGF through EEA1-positive endosomes. Previous studies showed that transferrin is not internalized through growth factor–induced macropinocytosis (Schnatwinkel et al., 2004), and consequently the uptake and trafficking of transferrin were not altered in the H-RasG12V–transformed cells (Supplemental Figure S7).

When investigating the activation of EGFR in H-RasG12V-transformed fibroblasts, we observed a modest but sustained increase in EGFR phosphorylation (Figure 5C), as previously demonstrated in H-Ras–transformed mammary epithelial cells (Martinez-Lacaci et al., 2000). The prolonged EGFR activation induced increased Erk1/2 phosphorylation, but it did not translate into sustained increase in activation of PI 3-kinase and PLCγ pathways (Figure 5C and Supplemental Figure S3). Furthermore, the EGFR phosphorylation was not affected by inhibition of PI 3-kinase in either wt or H-RasG12V–transformed fibroblasts (Supplemental Figure S8). These findings support the notion that macropinocytosis of PDGFRβ is at least partly responsible for the observed increase in amplitude and duration of receptor activation and downstream signaling.

Simultaneous PDGF-BB and EGF stimulation induces macropinocytosis of EGFR

As mentioned, macropinocytosis is dependent on PI 3-kinase activity. The observed receptor uptake through macropinocytosis (Figure 2A) correlated with an increased PI 3-kinase activity, as judged by Akt phosphorylation (Figure 1B), which may constitute either a cause or a consequence of the shift in receptor internalization pathway. It is therefore conceivable that receptor sorting into macropinosomes
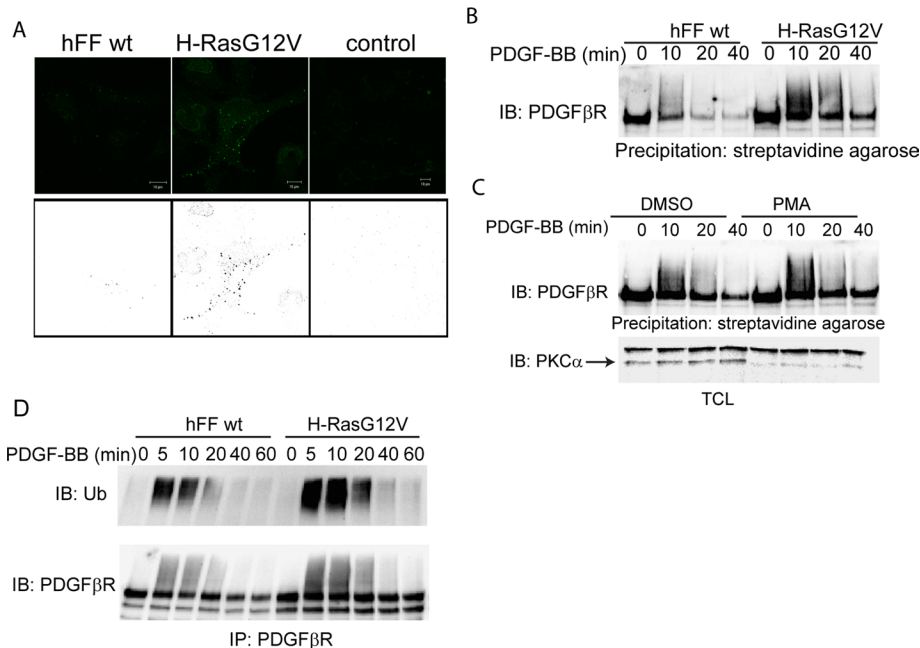
FIGURE 4: H-RasG12V transformation promotes PDGFRβ recycling. (A) Cells were incubated with a monoclonal antibody recognizing the extracellular domain of PDGFRβ at 37°C for 1 h. Antibody remaining at the cell surface was removed by acidic wash, followed by incubation with Alexa 488–conjugated anti-mouse antibody at 4 or 37°C for 1 h. After a second acid wash, cells were fixed, and internalized fluorescent antibodies, representing recycled receptors, were detected by confocal microscopy. As control, H-RasG12V–transformed fibroblasts were kept at 4°C during all incubations to inhibit membrane trafficking. (B) Cells were stimulated with 50 ng/ml PDGF-BB, and cell surface proteins were subsequently biotinylated using Sulfo-NHS-SS-Biotin. Biotinylated proteins, containing the cell surface receptor pool, were precipitated using streptavidin agarose. Precipitated proteins were separated by SDS–PAGE, and cell surface PDGFRβ was detected by immunoblotting. (C) H-RasG12V–transformed fibroblasts were treated overnight with 1 μM PMA to down-regulate protein kinase C or vehicle (0.01% DMSO), followed by stimulation with 50 ng/ml PDGF-BB. Cell surface proteins were subsequently biotinylated and precipitated using streptavidin agarose as described. Precipitated proteins were separated by SDS–PAGE and transferred to nitrocellulose filters, and the amount of cell surface PDGFRβ was determined by immunoblotting (top). Downregulation of PKC was confirmed by immunoblotting of total cell lysates for PKCα (bottom). Arrow indicates localization of PKCα protein band. (D) Serum-starved cells were stimulated with 50 ng/ml PDGF-BB for the indicated time periods, followed by lysis and immunoprecipitation of PDGFRβ. Precipitated receptors were separated by SDS–PAGE, and receptor ubiquitination was determined. The membranes were stripped and reprobed with a PDGFRβ antibody. Antibodies were visualized using ECL and a LAS-100plus CCD camera. Densitometric analysis of the immunoblots was performed using AIDA Advanced Image Data Analyzer software.

as a consequence of bulk plasma membrane uptake.

Costimulation with PDGF-BB and EGF increases the phosphorylation and macropinocytic uptake of both receptors in wt fibroblasts

When determining Akt phosphorylation on Thr308 as an indicator of PI 3-kinase activation, we observed that coactivation of EGFR and PDGFRβ induced a similar level of Akt activation in wt fibroblasts as that observed after activation of PDGFRβ in H-RasG12V–transformed fibroblasts. Therefore, if the PI 3-kinase activity is at least in part responsible for the switch in receptor uptake, we would predict that 1) coactivation of the EGFR and PDGFRβ causes receptor internalization through macropinocytosis also in wt fibroblasts, and 2) PIP$_3$ levels are higher after PDGF-BB stimulation on H-RasG12V–transformed fibroblasts. In agreement with our predictions, we found that also in wt fibroblasts costimulation with PDGF-BB and EGF caused internalization of both receptors through macropinocytosis (Figure 7, A–C). In addition, as indicated by Akt translocation, PDGF-BB caused a significantly larger accumulation of PIP$_3$ at the plasma membrane in Ras-transformed compared with wt fibroblasts (Figure 7D and Supplemental Figure S8). Of note, stimulation of wt fibroblasts with PDGF-BB and EGF significantly increased the PIP$_3$ levels in wt fibroblasts, reaching similar levels as after stimulation with PDGF-BB alone in Ras-transformed cells. This further supports the notion that the amplitude of PI 3-kinase activity regulates the uptake pathway of activated receptor tyrosine kinases. Also in wt fibroblasts, ligation of both receptors induced a large PI 3-kinase–dependent increase in PDGFRβ phosphorylation (Figure 7E). However, the effect on EGFR phosphorylation was less pronounced in these cells (Figure 7F) compared with H-RasG12V–transformed cells (Figure 6F).

DISCUSSION

In the present study, we show for the first time that fibroblast transformation by H-RasG12V induces internalization of PDGFRβ by macropinocytosis (Figure 2), which enhances its signaling activity (Figure 1B) and increases anchorage-independent proliferation (Figure 1A). Receptor internalization through macropinocytosis correlates with the level of PI 3-kinase activity (Figure 7D) and thus occurred also in wt fibroblasts after simultaneous activation of PDGFRβ and EGFR (Figure 7). These findings indicate that H-Ras transformation is enhanced by increased growth factor receptor signaling through receptor uptake via macropinocytosis.

Inhibition of macropinocytosis reduced the PDGFRβ phosphorylation in Ras-transformed cells (Figure 3A), whereas enhanced macropinocytosis through Rabankyrin-5 overexpression directly resulted in receptor hyperphosphorylation also in wt fibroblasts

is dependent on local levels of phosphatidylinositol (3,4,5)-trisphosphate (PIP$_3$). If so, the observed PI 3-kinase activity induced by EGF activation (Figure 5C) may be sufficient to trigger macropinocytosis but not the sorting of activated receptors into macropinosomes. To assess this notion, we investigated whether the PDGFRβ-induced PI 3-kinase activity in Ras-transformed fibroblasts would also cause macropinocytosis of activated EGFR. Simultaneous stimulation with PDGF-BB and EGF induced uptake of both PDGFRβ and EGFR into macropinosomes (Figure 6, A–C). This was associated with 1.8-fold increase in PDGFRβ phosphorylation after 20 min of stimulation (Figure 6D), which was reversed by PI 3-kinase inhibition (to 0.8-fold of PDGF-BB–treated cells). In addition, costimulation caused prolonged phosphorylation of EGFR (Figure 6E) and Akt (Figure 6F). In contrast, stimulation with PDGF-BB alone did not induce internalization of the EGFR (Figure 6B). This is an important finding, as it demonstrates that active receptor tyrosine kinases are sorted into macropinosomes through a selective process rather than being internalized

A

TR-dextran   EGFR   merge

+EGF
20 min

10 μm   10 μm   10 μm

B

Number of vesicles

800
600
400
200
0

—■— control
—◆— H-RasG12V

0 10 20 30 40 50 60
Time (min)

C

hFF wt   H-RasG12V

EGF (min) 0 5 10 20 40 60   0 5 10 20 40 60

IB:P-Tyr
IB:EGFR
IB:P-Akt
IB:Akt
IB:P-Erk
IB:Erk

TCL   TCL

IB:P-Tyr
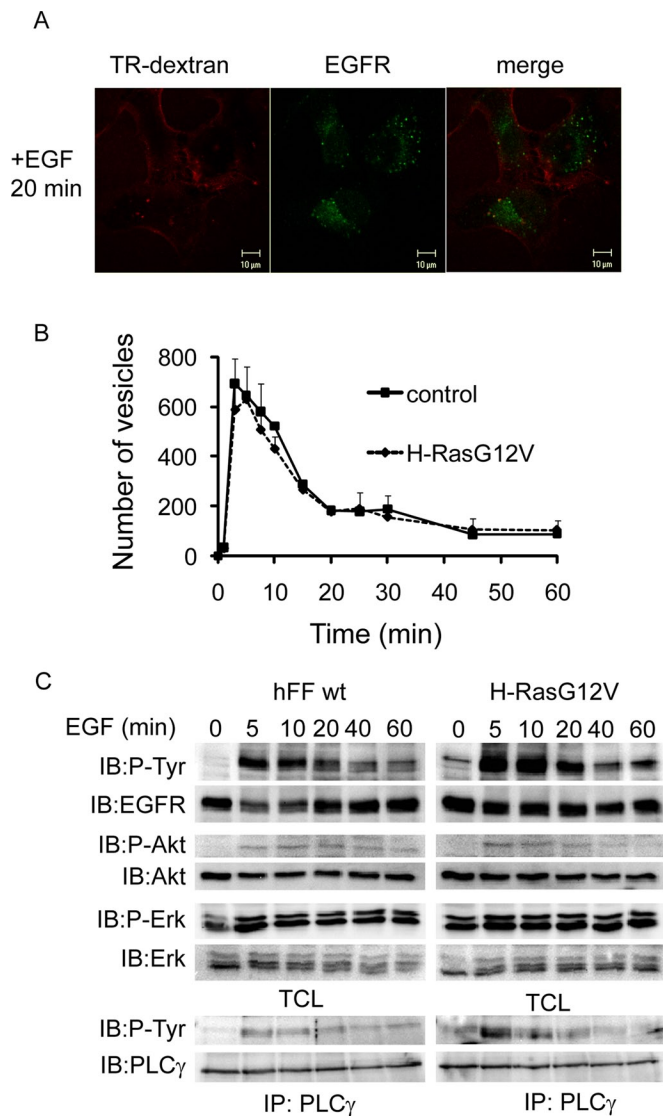IB:PLCγ

IP: PLCγ   IP: PLCγ

FIGURE 5: Activation of the EGFR is not affected by H-RasG12V transformation. (A) Serum-starved, H-RasG12V–transformed fibroblasts were stimulated with 50 ng/ml EGF for 20 min in the presence of 1 mg/ml Texas Red-dextran (MW, 70,000 Da). After washes with ice-cold PBS, the cells were fixed and stained with EGFR antibody (1:100). After mounting, the subcellular localization of the EGFR and macropinosomes was examined by confocal microscopy. (B) HeLa cells were transfected with GFP-H-RasG12V or GFP only (control). After 24 h, cells were stimulated with 100 ng/ml EGF–Alexa 555 for 1 min. The medium was replaced, and cells were incubated with 10 ng/ml EGF for the indicated time periods. After washes with ice-cold PBS, cells were fixed and stained with EEA1 antibody as a marker of early endosomes. After mounting, images were acquired using confocal microscopy. Colocalization between EEA1 and EGFR was calculated using the software MotionTracking as described in *Materials and Methods*. (C) Serum-starved cells were stimulated with 50 ng/ml EGF for the indicated time periods, and total cell lysates were collected. Where indicated, PLCγ was immunoprecipitated. Proteins were separated by SDS–PAGE, followed by immunoblotting using the indicated antibodies.

(Figure 3, C and D). This demonstrates that receptor uptake into macropinosomes is sufficient for enhanced PDGFRβ phosphorylation and downstream signaling. The mechanisms underlying the increased PDGFRβ activation after macropinocytosis are unclear. We previously

showed that PDGFRβ phosphorylation is primarily increased at the plasma membrane during receptor recycling (Karlsson et al., 2006). This suggests that the observed receptor recycling in Ras-transformed fibroblasts (Figure 4) is at least partially responsible for the enhanced receptor activation, possibly due to lower protein tyrosine phosphatase activity in the cell periphery (Reynolds et al., 2003). It is also possible that the observed increase in PI 3-kinase activity (Figure 7D) participates in the increased receptor activation, since PI 3-kinase activation downstream of PDGFRβ activates the NADPH oxidase (Persson et al., 2004b). This enhances the production of reactive oxygen species, which inhibit protein tyrosine phosphatases (Tonks, 2005). Macropinosomes may fuse with either early endosomes or the plasma membrane, but little is known about how the cargo modifies the fate of these vesicles. Although we observed receptor recycling (Figure 4), we also found that a pool of receptors rapidly localized to LAMP-1–positive compartments (Figure 2F). Given that we found that the rate of receptor degradation did not differ significantly between Ras-transformed and wt fibroblasts (Figure 2G), it is likely that the recycling pool is relatively small. These findings would be consistent with decreased intracellular phosphatase activity causing receptor hyperphosphorylation.

Several components of the signaling machinery activated downstream of receptor tyrosine kinases show distinct subcellular localization (Disanza et al., 2009; Murphy et al., 2009; Rodahl et al., 2009; Sadowski et al., 2009). In addition to attenuating signal transduction, endocytosis therefore provides spatiotemporal resolution of receptor signaling (Kholodenko, 2006). As previously described (Davies and Ross, 1978; West et al., 1989), activation of either PDGFRβ or EGFR triggered macropinocytosis in wt fibroblasts (Figure 7) but not sorting of activated receptors into macropinosomes (Figure 7C). Coactivation of PDGFRβ and EGFR increased the levels of PIP$_3$ generated (Figure 7D) and caused internalization of both receptors into macropinosomes (Figure 7C). Because Ras transformation caused enhanced PI 3-kinase activation in response to PDGF-BB, presumably via a direct interaction between H-RasG12V and PI 3-kinase (Karnoub and Weinberg, 2008), PDGFRβ was internalized through macropinocytosis (Figure 2). These data suggest that active sorting of receptors into macropinosomes constitutes a process by which cells increase their response to growth factors, possibly with the level of PIP$_3$ acting as sensor.

The notion of endocytosis providing spatial regulation of receptor signaling is supported by our findings that macropinocytosis of PDGFRβ enhanced the activation of both PLCγ/PKC and PI 3-kinase/Akt pathways but not of the Erk1/2 MAP kinase pathway (Figure 1B). Although many components of the molecular machinery that mediates endocytosis and receptor sorting have been elucidated, the regulatory mechanisms by which these components are used to fine tune receptor signaling remain poorly described (Mosesson et al., 2008). Activation of PKC has been shown to promote recycling of both EGFR (Bao et al., 2000) and PDGFRβ (Hellberg et al., 2009), resulting in delayed receptor degradation. In the present study, the increase in PKC activation was not required for the observed PDGFRβ recycling (Figure 4), confirming that PDGFRβ intracellular sorting occurs through a different pathway after H-RasG12V–induced macropinocytosis.

It is well established that mutations in the endocytic machinery that change the internalization and degradation of growth factor receptors can promote carcinogenesis (Bache et al., 2004; Mosesson et al., 2008). For example, the viral oncogene v-Cbl prevents ubiquitination and degradation of receptor tyrosine kinases, allowing for EGFR recycling (Levkowitz et al., 1998). Mutant p53 was recently shown to promote EGFR signal transduction by
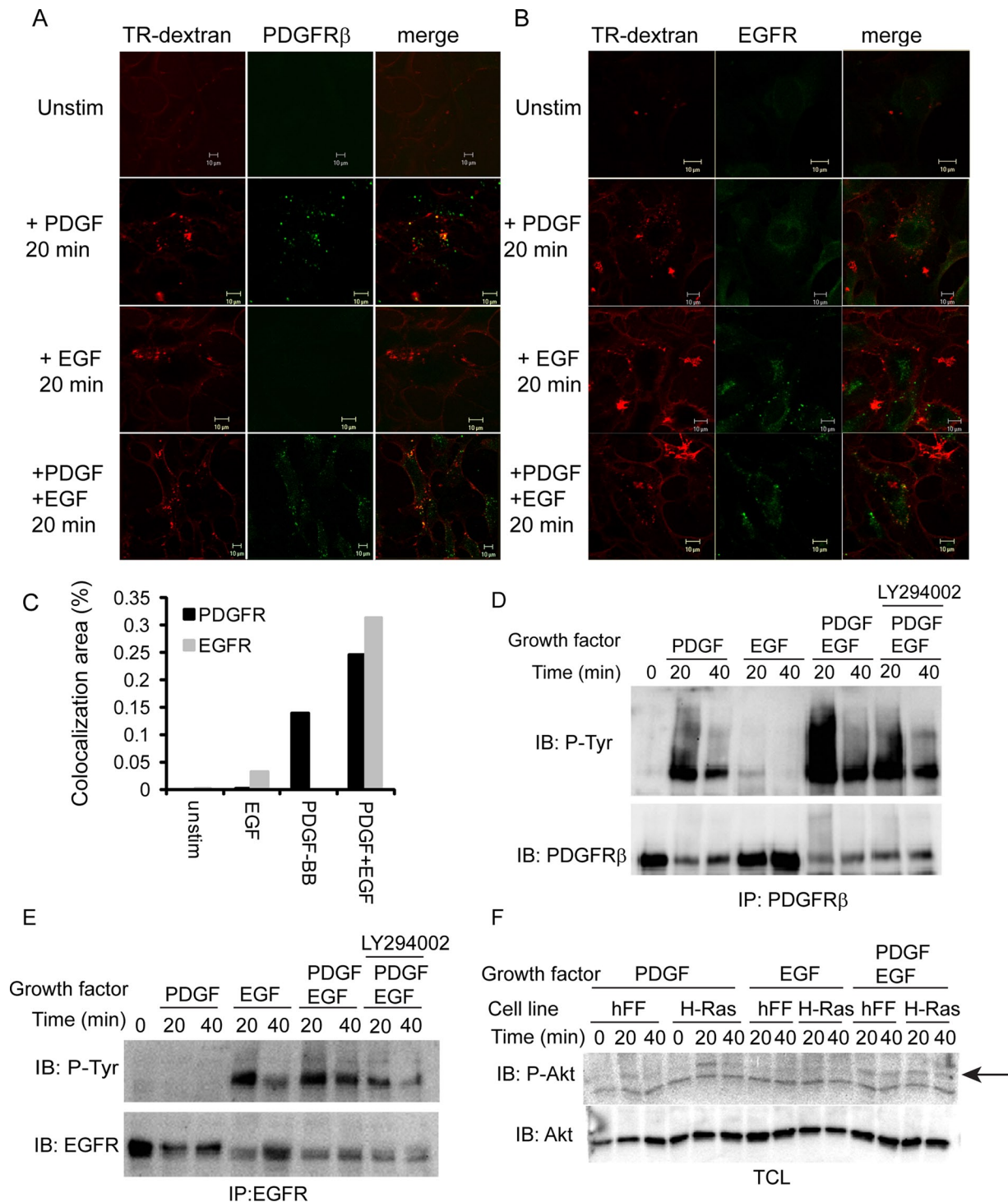
FIGURE 6: Coactivation of PDGFRβ and EGFR leads to macropinocytosis and increased phosphorylation of both receptors. H-RasG12V–transformed fibroblasts were incubated for 20 min with 1 mg/ml Texas Red-dextran (MW, 70,000 Da) in the presence or absence of 50 ng/ml PDGF-BB, 50 ng/ml EGF, or a combination of both growth factors. After washes with ice-cold PBS, the cells were fixed and stained with antibodies recognizing PDGFRβ (A) or EGFR (B). After mounting, the subcellular localization of the PDGF β-receptor and macropinosomes was examined by confocal microscopy. (C) Area of receptor and dextran colocalization in the images displayed in A and B, respectively, were quantified using ImageJ (National Institutes of Health, Bethesda, MD). (D) Serum-starved, H-RasG12V–transformed fibroblasts were treated with 25 μM LY294002 or vehicle (0.1% DMSO) for 15 min and stimulated with 50 ng/ml PDGF-BB and/or 50 ng/ml EGF for the indicated time periods. After cell lysis, the EGFR and PDGFRβ were sequentially immunoprecipitated, and the precipitated proteins were separated by SDS–PAGE. Phosphorylation of PDGFRβ (D) and EGFR (E) was determined using phosphotyrosine antibody, followed by stripping and reprobing with the indicated receptor antibody. (F) Serum-starved cells were treated with 25 μM LY294002 or vehicle (0.1% DMSO) for 15 min and stimulated with 50 ng/ml PDGF-BB (PDGF) and/or 50 ng/ml EGF for the indicated time periods. After cell lysis, total cell lysates were separated by SDS–PAGE. Phosphorylation of Akt was detected by immunoblotting, followed by stripping and reprobing with Akt antibody.
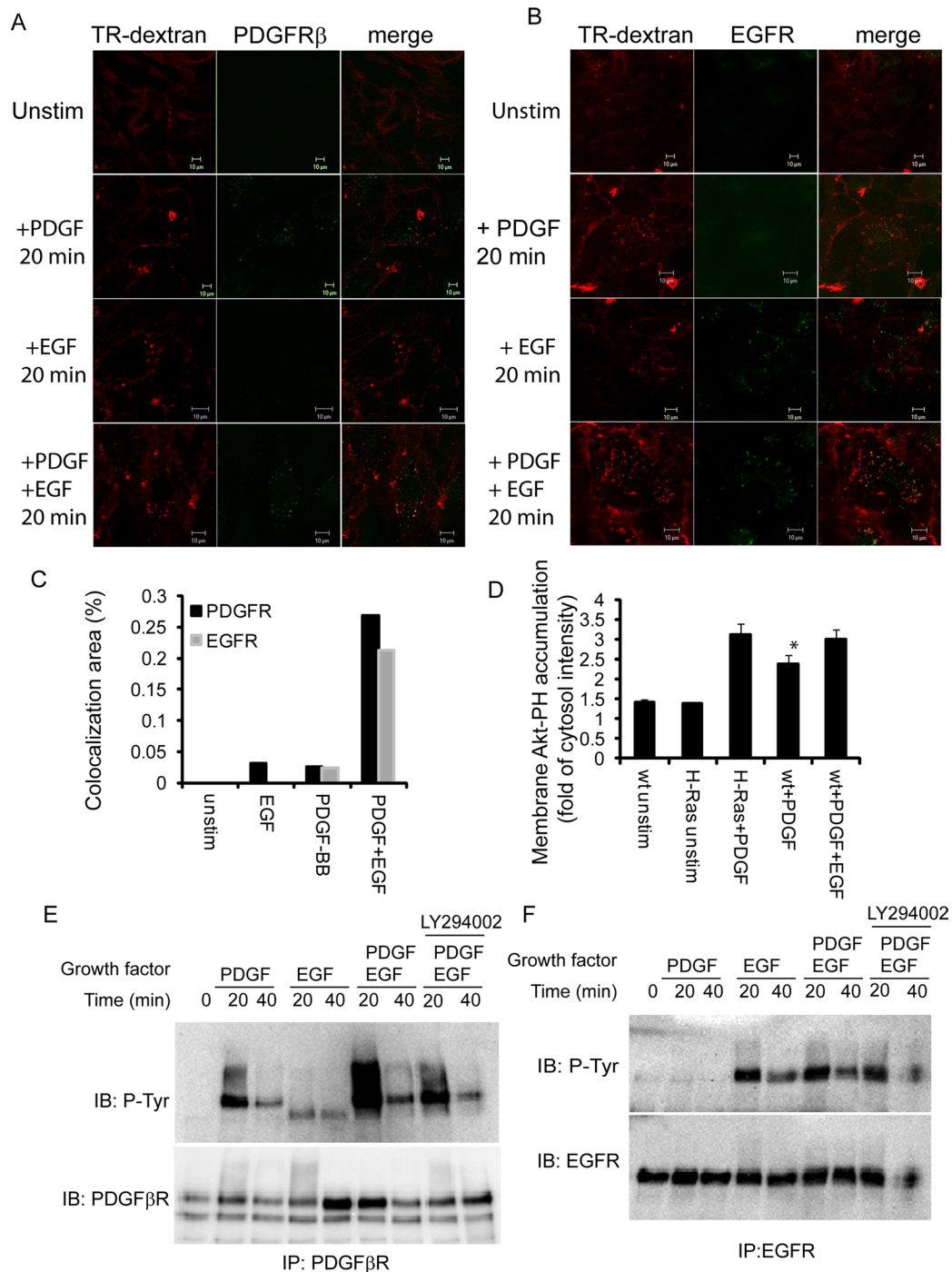
FIGURE 7: Coactivation of EGFR and PDGFRβ induce receptor uptake through macropinosomes in wt fibroblasts. Wild-type fibroblasts were incubated for 20 min with 1 mg/ml Texas Red-dextran (MW, 70,000 Da) in the presence or absence of 50 ng/ml PDGF-BB, 50 ng/ml EGF, or a combination of both growth factors. After washes with ice-cold PBS, the cells were fixed and stained with antibodies recognizing PDGFRβ (A) or EGFR (B). After mounting, the subcellular localization of the PDGF β-receptor and macropinosomes was examined by confocal microscopy. (C) Area of receptor and dextran colocalization in the images displayed in A and B, respectively, were quantified using ImageJ. (D) Cells were transfected with 0.5 μg of a plasmid expressing the PH domain of Akt labeled with YFP (YFP-Akt(PH)). After serum starvation, cells were stimulated with 50 ng/ml PDGF-BB and/or 50 ng/ml EGF for 5 min before fixation and image acquisition. The fold increase in YFP fluorescence at the plasma membrane was calculated as described in *Materials and Methods*. Quantifications were done in three independent replicates from a total of ~30 cells per condition. Statistically significant difference between Ras-transformed and wt cells stimulated with PDGF-BB was determined using unpaired Student's *t* test assuming equal variance: *$p < 0.05$. (E) Serum-starved wt fibroblasts were treated with 25 μM LY294002 or vehicle (0.1% DMSO) for 15 min and stimulated with 50 ng/ml PDGF-BB and/or 50 ng/ml EGF for the indicated time periods. After cell lysis, the EGFR and PDGFRβ were sequentially immunoprecipitated, and the precipitated proteins were separated by SDS–PAGE. Phosphorylation of PDGFRβ and EGFR (F) were determined using phosphotyrosine antibody, followed by stripping and reprobing with the indicated receptor antibody.

increasing the recycling of EGFR in complex with α5β1 integrin (Muller *et al.*, 2009). The present study shows that fibroblast transformation with H-RasG12V induces PDGFRβ internalization through macropinocytosis. This represents the first example of an oncogene that promotes a shift in endocytic pathways used by receptor tyrosine kinases. The finding that the ability of H-RasG12V to confer anchorage-independent cell proliferation was dependent on PDGFR activation (Figure 1A) is important, since it suggests that Ras-induced receptor macropinocytosis enhances the transformed phenotype. In this context, the observed increase in PDGF-induced Akt activation (Figure 1B) is of particular importance, since Akt signaling protects transformed cells from apoptosis (Carnero, 2010). Moreover, the notion that increased PI 3-kinase activity would promote increased receptor tyrosine kinase signaling would indicate that this mechanism could be of importance in tumors with activating mutations in PI 3-kinase or down-regulation of PTEN (Jiang and Liu, 2009).

In summary, our findings show that PDGFRβ internalization through macropinocytosis directly enhances receptor activity and downstream signaling. H-Ras transformation promotes receptor macropinocytosis, thereby enhancing transformed growth. These findings constitute the first evidence of an intracellular signaling pathway that regulates receptor tyrosine kinase activity by altering the endocytosis route.

MATERIALS AND METHODS

Antibodies and reagents

The following reagents were used: imatinib (a generous gift from Novartis, Basel, Switzerland), AG1296 (Sigma-Aldrich, St. Louis, MO), dynasore (Sigma-Aldrich), LY294002 (Santa Cruz Biotechnology, Santa Cruz, CA), human recombinant EGF (PeproTech, Rocky Hill, NJ), PDGF-BB (a generous gift from Amgen, Thousand Oaks, CA), Texas Red-dextran (molecular weight [MW], 70,000 Da, lysine fixable; Molecular Probes), EGF-Alexa 647 (Molecular Probes, Invitrogen, Carlsbad, CA), transferrin-Alexa 555 (Molecular Probes), and streptavidin agarose beads (GE Healthcare, Piscataway, NJ). The following antibodies were used for biochemical experiments: mouse anti-MARCKS, mouse anti-ubiquitin (P4G7), and mouse anti-phosphotyrosine (PY99) were from Santa Cruz Biotechnology. Mouse anti-PKCα and fluorescein isothiocyanate–mouse anti–LAMP-1 were from BD Biosciences (San Diego, CA). Rabbit anti–phospho-Akt (T308), rabbit anti-Akt, rabbit anti–phospho-MARCKS (Ser152/156), rabbit anti–phospho p44/42-MAPK (T202/Y204), rabbit anti-p44/42-MAPK, and rabbit anti-EGFR (D38B1) XP were from Cell Signaling Technology (Beverly, MA). Rabbit anti-PLCγ (Arteaga *et al.*, 1991), B2 mouse monoclonal anti–PDGF β-receptor (Rönnstrand *et al.*, 1988), rabbit anti–PDGF β-receptor (CTβ; Karlsson *et al.*, 2006), rabbit anti-hEEA1 (Rink *et al.*, 2005), rabbit anti–Rabankyrin-5 (Schnatwinkel *et al.*, 2004), and rabbit anti–phospho PDGF β-receptor Y579, Y581, Y716, Y751, Y763, Y771, Y778, Y857, Y1009, and Y1021 (Chiara *et al.*, 2004; Persson *et al.*, 2004a; Toffalini *et al.*, 2010) have been described. Plasmids containing the following fusion proteins were used: green fluorescent protein (GFP)–C1 (Clontech, Mountain View, CA), yellow fluorescent protein (YFP)–EGFR (P. Bastiaens, Max Planck Institute of Molecular Physiology, Dortmund, Germany), pEGFP-HRasG12V (Y. Kloog, Tel Aviv University, Tel Aviv, Israel), YFP-Akt(PH) (Shin *et al.*, 2005), and Rabankyrin5-YFP (Schnatwinkel *et al.*, 2004) were previously described.

Tissue culture and transfection

Wild-type human foreskin fibroblasts and fibroblasts transformed with H-RasG12V have been previously described (Hahn *et al.*, 1999).

All cells were grown in DMEM supplemented with 10% FBS, 100 U/ml penicillin, 100 μg/ml streptomycin, and 100 μg/ml amphotericin B. Before stimulation, the cells were serum starved overnight in DMEM containing penicillin/streptomycin and 1 mg/ml bovine serum albumin (BSA). Cells were transfected using JetPEI transfection reagent (PolyPlus-transfection SA, Illkirch, France), according to the manufacturer's protocol.

Soft agar colony formation assay

Colony formation in soft agar was determined by plating 2.5×10^4 H-RasG12V–transformed cells in 0.4 ml of DMEM supplemented with 100 U/ml penicillin, 100 μg/ml streptomycin, 100 μg/ml amphotericin B, 3% FBS, and 0.3% low–melting temperature agarose (Seaplaque; Lonza, Basel, Switzerland) in 12-well plates coated with 0.8 ml of 0.6% low–melting temperature agarose in the absence or presence of 50 ng/ml PDGF-BB and/or the PDGFR inhibitor AG1296 (2 μM) or imatinib (3 μM). Colony formation was monitored after 5 d of growth at 37°C, and colony number and size were recorded using an Axiovert 40 CFL microscope (Carl Zeiss, Göttingen, Germany).

Antibody recycling assay

Direct recycling was assayed based on a protocol described before (Mitchell *et al.*, 2004). Cells were seeded on Chamber Slides (Lab-Tek, Nalge Nunc International, Rochester, NY) and incubated with 2 μg/ml of the B2 PDGF β-receptor antibody at 4 or 37°C for 1 h. Any remaining surface antibody was removed by washing in DMEM and adjusted to pH 2.0 by HCl. Cells were then incubated with Alexa 488–conjugated anti-mouse antibody (diluted 1:1000) at 4 or 37°C for 1 h, followed by a second round of washing and acid stripping. Cultures were fixed, and internalized fluorescent antibodies, representing receptors that had recycled to the plasma membrane and been internalized a second time, were detected using a Zeiss 510 LSM with a 63×/1.4 numerical aperture objective.

Fluid-phase endocytosis of Texas Red–labeled dextran

Macropinocytosis of PDGFRβ and EGFR was followed as described previously (Amyere *et al.*, 2000), with some modifications. Briefly, cells grown on Chamber Slides were serum starved, followed by incubation with 1 mg/ml Texas Red-dextran (MW, 70,000 Da, lysine fixable) in starvation medium to fill macropinosomes. Cells were incubated in the presence or absence of 50 ng/ml PDGF-BB and/or 50 ng/ml EGF and LY-294002 (25 μM), as indicated, for 20 min at 37°C, transferred to ice, washed three times with ice-cold phosphate-buffered saline (PBS), and fixed with 4% paraformaldehyde (PFA) in PBS. PDGF β-receptor was detected by incubating cells with 2 μg/ml of the B2 monoclonal antibody raised against the extracellular domain of human PDGF β-receptor (Rönnstrand *et al.*, 1988), followed by an Alexa 488–conjugated secondary antibody (Invitrogen). A commercial rabbit polyclonal antibody (EGFR XP; Cell Signaling) was used to detect endogenous EGFR. The cells were mounted in Fluoromount G (Southern Biotechnology Associates, Birmingham, AL), and the subcellular localization of macropinosomes and the receptors were examined using a Zeiss 510 LSM equipped with a 63×/1.4 numerical aperture objective.

Detection of cell surface PDGF β-receptors

Cells were stimulated for the indicated time periods and then placed on ice to stop membrane trafficking. The cells were subsequently incubated with 0.5 mg/ml Sulfo-NHS-SS-Biotin (Pierce, Rockford, IL) in PBS, pH 8.0, for 1 h on ice. Unbound biotin was quenched by incubation in 50 mM Tris, pH 8.0, for 10 min on ice. The cells were rinsed twice in ice-cold PBS and lysed in 20 mM Tris-HCl, pH 7.5,

0.5% Triton X-100, 0.5% deoxycholate, 150 mM NaCl, 10 mM EDTA, 0.5 mM Na_3VO_4, and 75 KIU/ml aprotinin for 15 min on ice. The lysates were cleared by centrifugation at 13,000 rpm for 15 min at 4°C. Biotinylated proteins were precipitated with streptavidin agarose, and precipitated PDGF β-receptors were detected by enhanced chemiluminescence using a LAS-100plus charge-coupled device (CCD) camera (Fujifilm, Tokyo, Japan). Densitometric analysis of the bands was performed using AIDA Advanced Image Data Analyzer software (Raytest, Wilmington, NC).

Confocal analysis of PDGF β-receptor subcellular localization
Cells were seeded on Chamber Slides and transfected with dynamin K44A–GFP. After serum starvation, cells were stimulated with 50 ng/ml PDGF-BB, rinsed twice in PBS, and fixed with 4% paraformaldehyde in PBS, pH 7.3, as previously described (Burden-Gulley and Brady-Kalnay, 1999). The PDGF β-receptor was detected by incubating the cells with 5 μg/ml of PDGFRβ antibody (CTβ), followed by an Alexa 546–conjugated secondary antibody. After mounting in Fluoromount G, the subcellular localization of the PDGF β-receptor was examined using a Zeiss 510 LSM equipped with a 63×/1.4 numerical aperture objective.

Immunoprecipitation
Cells were starved overnight, followed by stimulation with 50 ng/ml PDGF-BB or 50 ng/ml EGF for different time periods. The cells were lysed as described, and the lysates were incubated with the indicated antibody for 1 h, followed by 1 h of incubation with protein A agarose (Pharmacia, GE Healthcare). The precipitated proteins were washed three times in lysis buffer. Proteins were separated by SDS–PAGE (7% polyacrylamide gel) and transferred to nitrocellulose membranes, which were incubated with the indicated antibodies. Bound antibodies were visualized by enhanced chemiluminescence (ECL). Densitometry analysis was performed as described. For detection of receptor ubiquitination, immunoprecipitated receptors were transferred to polyvinylidenedifluoride membranes, the membrane was preincubated in denaturing buffer (6 M guanidine-HCl, 20 mM Tris-HCl, pH 7.5, 5 mM β-mercaptoethanol, 1 mM phenyl methyl sulfonylfluoride) for 30 min at 4°C, washed six times in PBS, and blocked for 6 h with 5% BSA at room temperature. The membrane was then incubated overnight at 4°C with a mouse anti-ubiquitin antibody diluted in blocking buffer. Bound antibodies were visualized by ECL.

Endocytic transport assays
Cells grown on coverslips in 24-well plates were stimulated with 25 μg/ml transferrin–Alexa 647 and 100 ng/ml EGF–Alexa 555 or 50 ng/ml PDGF-BB and 100 ng/ml EGF–Alexa 647 in CO_2-independent medium for 1 min at 37°C. Alternatively, the cells were stimulated for 10 min with 50 ng/ml PDGF-BB and 1 mg/ml Texas Red-dextran (MW, 70,000 Da, lysine fixable). Afterward, medium was removed and exchanged with 250 μg/ml Holo-Transferrin (Sigma-Aldrich) and 10 ng/ml EGF in CO_2-independent medium or CO_2-independent medium only. Incubation proceeded at 37°C for the indicated time periods. The cells were then washed with ice-cold PBS and fixed with 4% PFA. Immunostainings were performed as described previously (Rink et al., 2005), and coverslips were mounted on Mowiol. Images were acquired with a Zeiss 510 LSM with a 63×/1.4 numerical aperture objective. Image analysis was performed on the maximum projection of four z-planes. Background subtraction and vesicle fitting using MotionTracking were done as described previously (Rink et al., 2005). Colocalization was measured on basis of cross-sectional overlap, scoring >40%

overlap as colocalized. The vesicle size corresponds to the radius (in microns) of the apparent fluorescent area of an endosome (above the half-maximum value of fluorescence intensity of each structure).

PIP_3 measurements
HFF RasG12V or WT cells were transfected with 0.5 μg of a plasmid expressing the PH domain of Akt labeled with YFP (YFP-Akt(PH)). Twenty-four hours after transfection, cells were starved for 24 h before stimulation for 5 min with 50 ng/ml PDGF alone or together with 50 ng/ml EGF before fixation and image acquisition. To quantify the levels of PIP_3 after growth factor stimulation per cell, we calculated the YFP-Akt(PH) intensity profile along a line drawn "perpendicular" to the cell margin and spanning the whole cell (see Supplemental Figure S8). The fold increase in YFP fluorescence was calculated by dividing the maximum peak in intensity profile by the mean cytosolic YFP intensity. Quantifications were done in three independent replicates from a total of ~30 cells per condition.

REFERENCES
Amyere M, Payrastre B, Krause U, Van Der Smissen P, Veithen A, Courtoy PJ (2000). Constitutive macropinocytosis in oncogene-transformed fibroblasts depends on sequential permanent activation of phosphoinositide 3-kinase and phospholipase C. Mol Biol Cell 11, 3453–3467.

Andrae J, Gallini R, Betsholtz C (2008). Role of platelet-derived growth factors in physiology and medicine. Genes Dev 22, 1276–1312.

Arteaga CL, Johnson MD, Todderud G, Coffey RJ, Carpenter G, Page DL (1991). Elevated content of the tyrosine kinase substrate phospholipase C-gamma 1 in primary human breast carcinomas. Proc Natl Acad Sci USA 88, 10435–10439.

Bache KG, Slagsvold T, Stenmark H (2004). Defective downregulation of receptor tyrosine kinases in cancer. EMBO J 23, 2707–2712.

Bao J, Alroy I, Waterman H, Schejter ED, Brodie C, Gruenberg J, Yarden Y (2000). Threonine phosphorylation diverts internalized epidermal growth factor receptors from a degradative pathway to the recycling endosome. J Biol Chem 275, 26178–26186.

Bar-Sagi D, Feramisco JR (1986). Induction of membrane ruffling and fluid-phase pinocytosis in quiescent fibroblasts by ras proteins. Science 233, 1061–1068.

Burden-Gulley SM, Brady-Kalnay SM (1999). PTPmu regulates N-cadherin-dependent neurite outgrowth. J Cell Biol 144, 1323–1336.

Calzolari F, Malatesta P (2010). Recent insights into PDGF-induced gliomagenesis. Brain Pathol 20, 527–538.

Carnero A (2010). The PKB/AKT pathway in cancer. Curr Pharmaceut Des 16, 34–44.

Chen KT, Lin JD, Liou MJ, Weng HF, Chang CA, Chan EC (2006). An aberrant autocrine activation of the platelet-derived growth factor alpha-receptor in follicular and papillary thyroid carcinoma cell lines. Cancer Lett 231, 192–205.

Chiara F, Goumans MJ, Forsberg H, Ahgren A, Rasola A, Aspenstrom P, Wernstedt C, Hellberg C, Heldin CH, Heuchel R (2004). A gain of function mutation in the activation loop of platelet-derived growth factor beta-receptor deregulates its kinase activity. J Biol Chem 279, 42516–42527.

Davies PF, Ross R (1978). Mediation of pinocytosis in cultured arterial smooth muscle and endothelial cells by platelet-derived growth factor. J Cell Biol 79, 663–671.

Disanza A, Frittoli E, Palamidessi A, Scita G (2009). Endocytosis and spatial restriction of cell signaling. Mol Oncol 3, 280–296.

Downward J (2003). Targeting RAS signalling pathways in cancer therapy. Nat Rev 3, 11–22.

Eyster CA, Higginson JD, Huebner R, Porat-Shliom N, Weigert R, Wu WW, Shen RF, Donaldson JG (2009). Discovery of new cargo proteins

that enter cells through clathrin-independent endocytosis. Traffic 10, 590–599.

Fischer AN, Fuchs E, Mikula M, Huber H, Beug H, Mikulits W (2007). PDGF essentially links TGF-beta signaling to nuclear beta-catenin accumulation in hepatocellular carcinoma progression. Oncogene 26, 3395–3405.

Frederick L, Wang XY, Eley G, James CD (2000). Diversity and frequency of epidermal growth factor receptor mutations in human glioblastomas. Cancer Res 60, 1383–1387.

Gotzmann J et al. (2006). A crucial function of PDGF in TGF-beta-mediated cancer progression of hepatocytes. Oncogene 25, 3170–3185.

Hahn WC, Counter CM, Lundberg AS, Beijersbergen RL, Brooks MW, Weinberg RA (1999). Creation of human tumour cells with defined genetic elements. Nature 400, 464–468.

Hellberg C, Schmees C, Karlsson S, Ahgren A, Heldin CH (2009). Activation of protein kinase C alpha is necessary for sorting the PDGF beta-receptor to Rab4a-dependent recycling. Mol Biol Cell 20, 2856–2863.

Hermanson M, Funa K, Hartman M, Claesson-Welsh L, Heldin CH, Westermark B, Nister M (1992). Platelet-derived growth factor and its receptors in human glioma tissue: expression of messenger RNA and protein suggests the presence of autocrine and paracrine loops. Cancer Res 52, 3213–3219.

Hewlett LJ, Prescott AR, Watts C (1994). The coated pit and macropinocytic pathways serve distinct endosome populations. J Cell Biol 124, 689–703.

Jechlinger M, Sommer A, Moriggl R, Seither P, Kraut N, Capodiecci P, Donovan M, Cordon-Cardo C, Beug H, Grunert S (2006). Autocrine PDGFR signaling promotes mammary cancer metastasis. J Clin Invest 116, 1561–1570.

Jiang BH, Liu LZ (2009). PI3K/PTEN signaling in angiogenesis and tumorigenesis. Adv Cancer Res 102, 19–65.

Karlsson S, Kowanetz K, Sandin A, Persson C, Ostman A, Heldin CH, Hellberg C (2006). Loss of T-cell protein tyrosine phosphatase induces recycling of the platelet-derived growth factor (PDGF) beta-receptor but not the PDGF alpha-receptor. Mol Biol Cell 17, 4846–4855.

Karnoub AE, Weinberg RA (2008). Ras oncogenes: split personalities. Nat Rev Mol Cell Biol 9, 517–531.

Kerr MC, Lindsay MR, Luetterforst R, Hamilton N, Simpson F, Parton RG, Gleeson PA, Teasdale RD (2006). Visualisation of macropinosome maturation by the recruitment of sorting nexins. J Cell Sci 119, 3967–3980.

Kerr MC, Teasdale RD (2009). Defining macropinocytosis. Traffic 10, 364–371.

Kholodenko BN (2006). Cell-signalling dynamics in time and space. Nat Rev Mol Cell Biol 7, 165–176.

Koumakpayi IH, Le Page C, Delvoye N, Saad F, Mes-Masson AM (2011). Macropinocytosis inhibitors and Arf6 regulate ErbB3 nuclear localization in prostate cancer cells. Mol Carcinog 50, 901–912.

Levkowitz G, Waterman H, Zamir E, Kam Z, Oved S, Langdon WY, Beguinot L, Geiger B, Yarden Y (1998). c-Cbl/Sli-1 regulates endocytic sorting and ubiquitination of the epidermal growth factor receptor. Genes Dev 12, 3663–3674.

Martinez-Lacaci I, Kannan S, De Santis M, Bianco C, Kim N, Wallace-Jones B, Ebert AD, Wechselberger C, Salomon DS (2000). RAS transformation causes sustained activation of epidermal growth factor receptor and elevation of mitogen-activated protein kinase in human mammary epithelial cells. Int J Cancer 88, 44–52.

Mayor S, Pagano RE (2007). Pathways of clathrin-independent endocytosis. Nat Rev Mol Cell Biol 8, 603–612.

Mitchell H, Choudhury A, Pagano RE, Leof EB (2004). Ligand-dependent and -independent transforming growth factor-beta receptor recycling regulated by clathrin-mediated endocytosis and Rab11. Mol Biol Cell 15, 4166–4178.

Mitin N, Rossman KL, Der CJ (2005). Signaling interplay in Ras superfamily function. Curr Biol 15, R563–574.

Mosesson Y, Mills GB, Yarden Y (2008). Derailed endocytosis: an emerging feature of cancer. Nat Rev 8, 835–850.

Muller PA et al. (2009). Mutant p53 drives invasion by promoting integrin recycling. Cell 139, 1327–1341.

Murphy JE, Padilla BE, Hasdemir B, Cottrell GS, Bunnett NW (2009). Endosomes: a legitimate platform for the signaling train. Proc Natl Acad Sci USA 106, 17615–17622.

Persson C et al. (2004a). Site-selective regulation of platelet-derived growth factor beta receptor tyrosine phosphorylation by T-cell protein tyrosine phosphatase. Mol Cell Biol 24, 2190–2201.

Persson C, Sjoblom T, Groen A, Kappert K, Engstrom U, Hellman U, Heldin CH, den Hertog J, Ostman A (2004b). Preferential oxidation of the second phosphatase domain of receptor-like PTP-alpha revealed by an antibody against oxidized protein tyrosine phosphatases. Proc Natl Acad Sci USA 101, 1886–1891.

Peschard P, Park M (2003). Escape from Cbl-mediated downregulation: a recurrent theme for oncogenic deregulation of receptor tyrosine kinases. Cancer Cell 3, 519–523.

Petiot A, Faure J, Stenmark H, Gruenberg J (2003). PI3P signaling regulates receptor sorting but not transport in the endosomal pathway. J Cell Biol 162, 971–979.

Porat-Shliom N, Kloog Y, Donaldson JG (2008). A unique platform for H-Ras signaling involving clathrin-independent endocytosis. Mol Biol Cell 19, 765–775.

Reynolds AR, Tischer C, Verveer PJ, Rocks O, Bastiaens PI (2003). EGFR activation coupled to inhibition of tyrosine phosphatases causes lateral signal propagation. Nat Cell Biol 5, 447–453.

Rink J, Ghigo E, Kalaidzidis Y, Zerial M (2005). Rab conversion as a mechanism of progression from early to late endosomes. Cell 122, 735–749.

Rodahl LM, Stuffers S, Lobert VH, Stenmark H (2009). The role of ESCRT proteins in attenuation of cell signalling. Biochem Soc Trans 37, 137–142.

Roepstorff K, Grovdal L, Grandal M, Lerdrup M, van Deurs B (2008). Endocytic downregulation of ErbB receptors: mechanisms and relevance in cancer. Histochem Cell Biol 129, 563–578.

Rönnstrand L, Terracio L, Claesson-Welsh L, Heldin CH, Rubin K (1988). Characterization of two monoclonal antibodies reactive with the external domain of the platelet-derived growth factor receptor. J Biol Chem 263, 10429–10435.

Sadowski L, Pilecka I, Miaczynska M (2009). Signaling from endosomes: location makes a difference. Exp Cell Res 315, 1601–1609.

Schnatwinkel C, Christoforidis S, Lindsay MR, Uttenweiler-Joseph S, Wilm M, Parton RG, Zerial M (2004). The Rab5 effector Rabankyrin-5 regulates and coordinates different endocytic mechanisms. PLoS Biol 2, E261.

Shin HW et al. (2005). An enzymatic cascade of Rab5 effectors regulates phosphoinositide turnover in the endocytic pathway. J Cell Biol 170, 607–618.

Slamon DJ, Clark GM, Wong SG, Levin WJ, Ullrich A, McGuire WL (1987). Human breast cancer: correlation of relapse and survival with amplification of the HER-2/neu oncogene. Science 235, 177–182.

Swanson JA, Watts C (1995). Macropinocytosis. Trends Cell Biol 5, 424–428.

Toffalini F, Hellberg C, Demoulin JB (2010)Critical role of the platelet-derived growth factor receptor (PDGFR) beta transmembrane domain in the TEL-PDGFRbeta cytosolic oncoprotein. J Biol Chem 285, 12268–12278.

Tonks NK (2005). Redox redux: revisiting PTPs and the control of cell signaling. Cell 121, 667–670.

West MA, Bretscher MS, Watts C (1989). Distinct endocytotic pathways in epidermal growth factor-stimulated human carcinoma A431 cells. J Cell Biol 109, 2731–2739.

Zwick E, Bange J, Ullrich A (2001). Receptor tyrosine kinase signalling as a target for cancer intervention strategies. Endocr Relat Cancer 8, 161–173.